

Investigation of Al-Fe-Si Alloys with Additions of Hf, Sc and Zr

H. Hallem, B. Forbord, K. Marthinsen

Department of Materials Technology, Faculty of Natural Sciences and Technology, 7491 Trondheim, Norway.

Keywords: Al₃Hf, Al₃(Hf,Sc), Al₃(Hf,Zr), Extrusion, Recrystallisation resistance.

Abstract

To meet the demand for extruded aluminium alloys tolerant of exposures to high temperatures (~600°C), highly stable microstructures are required. In order to achieve this, Hf, Sc and Zr were added to Al-Fe-Si alloys. These elements form dispersoids of the type Al₃X (X=Hf,Sc,Zr) in aluminium alloys, and Transmission Electron Microscopy (TEM) has been applied in order to gain more information about the formation of these phases. The recrystallisation resistance during extrusion and subsequent annealing was also investigated. Al-Fe-Si with Hf, Sc and Zr displayed a remarkable recrystallisation resistance as only a thin surface layer recrystallised during post-extrusion annealing at 600°C. The variant containing only Hf was far less resistant towards recrystallisation as it recrystallised completely already during extrusion.

1. Introduction

As recrystallisation is connected with a considerable loss in strength, dispersoid forming elements are added to aluminium alloys in order to slow down/inhibit this process. Recrystallisation involves the formation of strain-free nuclei/subgrains and the subsequent growth of these into the surrounding matrix in a heavily deformed material. However, the formation of recrystallised grains will only occur if the subgrains are able to grow larger than a certain size, R_C . This is described mathematically by the Gibbs-Thomson relationship

$$R > R_C = \frac{4 \cdot \gamma_{GB}}{P_D - P_Z} \quad (1)$$

where R_C is the critical radius for nucleation, γ_{GB} is the specific grain boundary energy and P_D is the stored deformation energy. P_Z is the retarding force (usually referred to as the Zener drag) that the dispersoids exert upon the subgrain boundaries. This should be as large as possible in order to achieve a high recrystallisation resistance, see Eq. 1. A widely used estimate for the Zener drag is [1]:

$$P_Z = \frac{3 \cdot f \cdot \gamma_{GB}}{2 \cdot r} \quad (2)$$

where r is the radius and f is the volume fraction of dispersoids. Eq. 2 shows that a high volume fraction of small dispersoids is necessary in order to achieve a large Zener-drag and a high recrystallisation resistance.

In this work Hf, Sc and Zr, both alone and in combination, have been added to a commercially pure Al-alloy. These elements form Al_3X -dispersoids ($X=Hf,Sc,Zr$) during annealing, and the objective has been to find the optimum combined addition of these elements with respect to recrystallisation resistance. At a later stage such additions will be tried in a commercial Al-Mn-alloy.

2. Experimental

2.1 Casting

The alloys were produced by mixing appropriate amounts of Vigeland metal (99, 999% Al), master alloys of Al-5wt%Hf, Al-2wt%Sc, Al-10wt%Zr, Al-10wt%Si and small Fe pellets. The alloys were directionally solidified in order to reduce porosity and solidification contraction at the top. A well stirred melt was poured at 760°C into a cylindrical fibre tube mould ($\varnothing 100\text{mm} \times 200\text{mm}$) cooled at the bottom by a jet of water. The actual temperature was monitored by thermocouples during solidification. As a precaution a minimum of 10mm from the top and 5mm from the bottom of each ingot were cut off and scrapped to avoid any edge effects during subsequent thermo-mechanical processing. Following preheating approximately 2mm of the outer surface were removed using a lathe reducing the diameter to 100mm. The billets were finally cut in lengths of 150mm.

2.2 Homogenisation.

All alloys were homogenised in a Heraeus K750 air-circulating furnace for 5-20hr at 475°C. A heating rate of 50°C/hr was applied. An external reference thermocouple was used in order to monitor the temperature in the oven during the heat treatment.

2.3 Extrusion

Ingots were heated to the extrusion temperature (480°C) within 3 min by an induction heater and then quickly transferred to the extrusion container. Extrusion profiles with dimensions 1.9mm x 39.9mm were produced at a ram speed of 6mm/s. Thermocouples were used in order to monitor the profile temperature during extrusion. The ram pressure was also recorded continuously during extrusion.

2.4 Annealing

Annealing after extrusion was performed in a salt bath in order to ensure rapid upquenching. Thermal stability of this bed was better than $\pm 2^\circ\text{C}$. All samples were quenched in water.

2.5 Compositional Analysis

The alloy compositions were determined by a JEOL JXA-8900M microprobe equipped with WDS (Wavelength Dispersive Spectrometry). XRF analysis and a Baird Spectrovac optical emission spectrograph were also used for comparison. Compositional analyses are shown in table 1.

2.6 Optical Microscopy

Samples for optical microscopy were taken from the centreline of the extruded profile in the direction of extrusion and polished in the usual manner. The entire cross section was available for inspection. Samples were anodised at an applied voltage of 20VDC using an electrolyte consisting of 0.5L of H₂O, 2.3ml fluoboric acid, and 3.5g boric acid. Polarised light was then used in the investigation of the grain structure.

2.7 TEM/EELS/EDS

A Jeol 2010 operated at 200 kV was used in the TEM-investigations. EELS (Electron Energy Loss Spectrum) was used in order to measure the thickness of the TEM-foils, and dispersoid sizes, number densities and volume fractions were subsequently determined from dark field images analysed by the computer programs Adobe PhotoShop and ImageTool. 500-1000 dispersoids were measured/counted in each sample. In alloys where a heterogeneous dispersoid distribution was observed, maximum number densities were calculated. EDS (Energy Dispersive Spectrometry) was used in order to investigate the chemical composition of the dispersoids. During the analyses a focused nano-beam (spot size 5-10 nm) was placed directly on the dispersoids. Analyses of the surrounding matrix were also performed in order to eliminate the matrix contribution to the dispersoid spectra.

3. Results and Discussion

Table 1: Chemical composition of the alloys.

Alloy 1	
WDS	Al-0,61Hf-0,14Si-0,15Fe
XRF	Al-0,64Hf-0,15Si-0,19Fe
Spec	Al-XHf-0,17Si-0,22Fe
Alloy 2	
WDS	Al-0,46Hf-0,10Zr-0,13Si-0,19Fe
XRF	Al-0,47Hf-0,12Zr-0,13Si-0,2Fe
Spec	Al-XHf-0,12Zr-0,15Si-0,21Fe
Alloy 3	
WDS	Al-0,52Hf-0,16Sc-0,16Si-0,21Fe
XRF	Al-0,57Hf-0,17Sc-0,14Si-0,2Fe
Spec	Al-XHf-XSc-0,17Si-0,22Fe
Alloy 4	
WDS	Al-0,51Hf-0,16Sc-0,06Zr-0,14Si-0,22Fe
XRF	Al-0,51Hf-0,17Sc-0,05Zr-0,15Si-0,2Fe
Spec	Al-XHf-XSc-0,05Zr-0,17Si-0,22Fe

XRF: Standardless/semiquantitative measurement in X-ray spectrometer.

Spec: Spark spectrograph.

WDS: Microprobe, WDS.

3.1 Chemical Composition

Table 1 shows the chemical composition [wt%] of the alloys determined by the methods mentioned in the previous chapter. Spark spectrograph is unable to measure Hf or Sc, and the composition has therefore been replaced with an X in the table. It is important to notice

that the different techniques used in the analysis of the chemical composition (XRF, WDS and spectrograph) gave virtually similar results. The compositions found in WDS was chosen as all elements can be measured by this method.

Table 2: Technical details from the extrusion.

Alloy	Max temp. (°C)	Max extr. force (kN)	Extr. speed (mm/s)	Pre-heating (°C)
1.Al-Hf-Si-Fe	533	2562	6,1	477
2.Al-Hf-Zr-Si-Fe	552	2926	6,1	480
3.Al-Hf-Sc-Si-Fe	572	3886	6,1	475
4.Al-Hf-Sc-Zr-Si-Fe	578	4216	6,1	480

3.2 Extrudability:

Table 2 shows that the maximum temperature varies between 533°C-578°C during extrusion and alloy 4, which has the highest content of alloying elements, reaches the highest temperature. The maximum extrusion force also increases with the amount of alloying elements. As will be shown this is due to the formation of dispersoids, which increases the deformation resistance of the alloy, but despite the presence of these dispersoids the extrusion pressure is not very high. However, other alloying elements like for instance Mn would have increased the extrusion pressure considerably, and as one of the long term objectives of this investigation is to develop a commercial Al-Mn alloy, the high dispersoid density may eventually cause problems with respect to the extrudability.

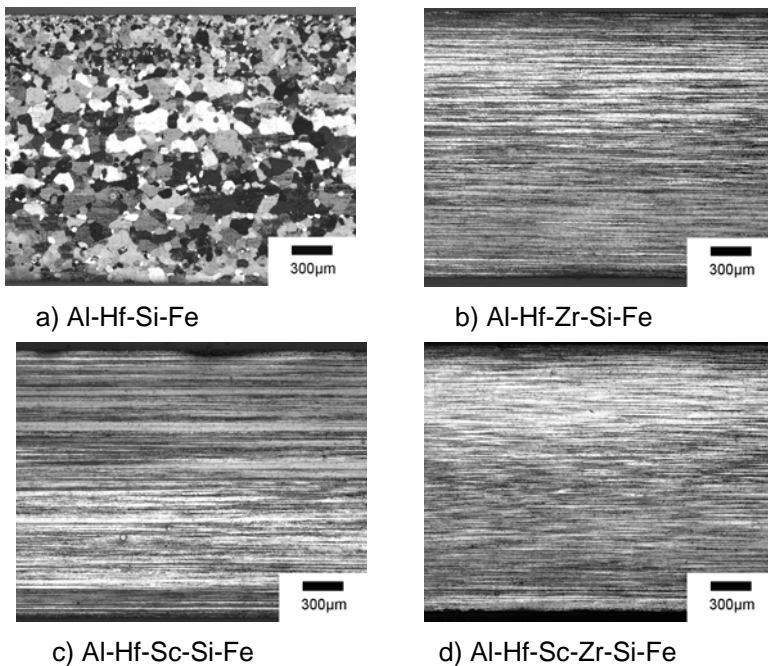


Figure 1: Anodised micrographs of the as extruded material.

The micrographs in figure 1 show that alloy 1 has recrystallised completely during extrusion. The main reason for the low recrystallisation resistance of this alloy is the low number density of Al_3Hf . In an earlier investigation Ryum [2] showed that precipitation of Hf is a slow process, but Hori et al [3] and Hallem et al [4] both showed that Si facilitates the precipitation of Al_3Hf . However, as Fe also is present in this alloy, some of the Si enters Al-Si-Fe-precipitates instead of enhancing Al_3Hf formation.

The extruded profiles of alloys 2-4, on the other hand, showed no signs of recrystallisation. This is due to the dramatic increase in dispersoid density when Zr and Sc are added, see Figs.2a-c. EDS/TEM revealed that the dispersoids were of the type $Al_3(Hf,Zr)$, $Al_3(Hf,Sc)$ and $Al_3(Hf,Sc,Zr)$ in alloys 2-4, respectively. Their respective average radii were 14nm, 9nm and 7nm, respectively.

It is also important to notice that the width of the dispersoid size distribution decreases with the total amount of (Hf+Sc+Zr). In alloy 4, which contains all these elements, a narrow particle size distribution was observed. This may indicate that the $Al_3(Hf,Sc,Zr)$ dispersoids nucleate almost simultaneously. This is shown in Table 3 and Figure 3.

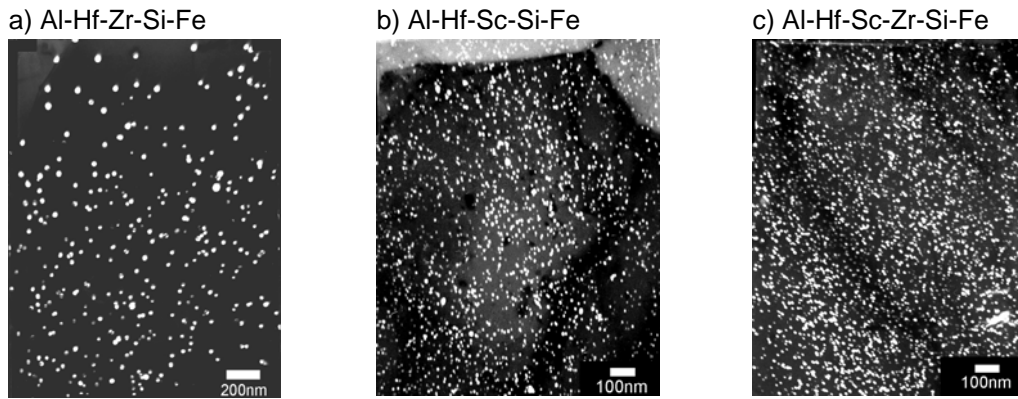


Figure 2: Dark Field TEM micrographs of dispersoids a) $\text{Al}_3(\text{Hf},\text{Zr})$ b) $\text{Al}_3(\text{Hf},\text{Sc})$ c) $\text{Al}_3(\text{Hf},\text{Sc},\text{Zr})$.

Table 3: Average radius, maximum density and volume fraction after extrusion.

Alloy	Average radius/ St.dev	Max Density [m^3]	Average Density [m^3]	Average volume fraction
1. Al-Hf-Si-Fe	Too few to measure	-	-	-
2. Al-Hf-Zr-Si-Fe*	13,8nm/3,5nm	2,54E+21	9,13E+20	-
3. Al-Hf-Sc-Si-Fe	8,7nm/2,8nm	1,08E+22	4,51E+21	1,24E-02
4. Al-Hf-Sc-Zr-Si-Fe	7,1nm/1,1nm	1,67E+22	1,39E+22	2,08E-02

*Due to heterogeneous distribution, the average volume fraction of this variant was not measured.

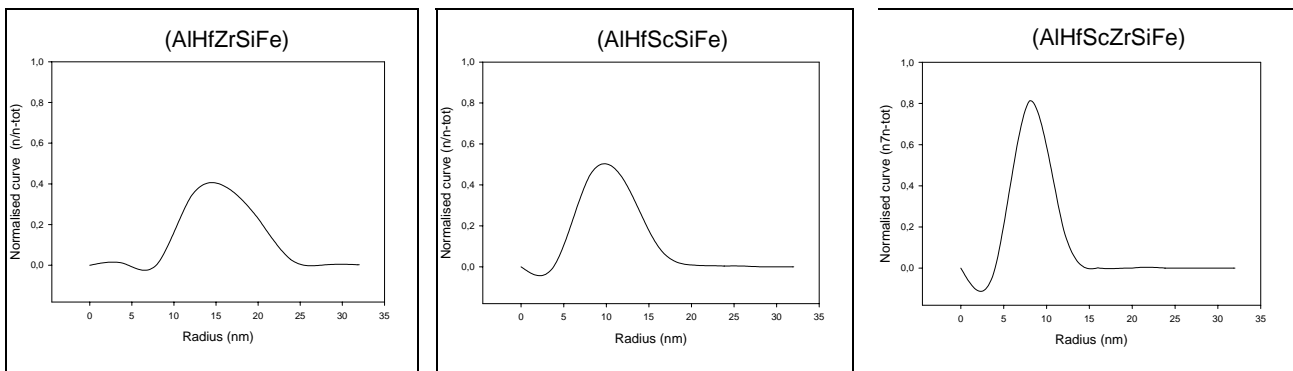


Figure 3: Dispersoid size distributions for alloys 2-4. Both the average radius and the width of the distribution decreases with increasing amount of (Hf+Sc+Zr).

Table 4: Recrystallisation performance of the alloys.

Alloy	Homogenisation	Temperature	Microstructure
1. Al-Hf-Si-Fe	50C/hr +20hr at 475C	As extruded 500C 550C 600C	Recrystallised - - -
2. Al-Hf-Zr-Si-F	50C/hr +20hr at 475C	As extruded 500C 550C 600C	Unrecrystallised Unrecrystallised Recrystallised Recrystallised
3. Al-Hf-Sc-Si-Fe	50C/hr +5hr at 475C	As extruded 500C 550C 600C	Unrecrystallised Unrecrystallised Unrecrystallised Recrystallised
4. Al-Hf-Sc-Zr-Si-Fe	50C/hr +5hr at 475C	As extruded 500C 550C 600C	Unrecrystallised Unrecrystallised Unrecrystallised Surface Recrystallised

3.3 Post Extrusion Annealing

The recrystallisation performance of the extruded profiles of alloy 2-4 was also investigated. In alloy 2 no signs of recrystallisation could be seen at 500°C, but after 1hr annealing at 550°C it was fully recrystallised. Alloy 3 performed even better as it stayed unrecrystallised at 550°C, but during annealing at 600°C it recrystallised completely. However, when Hf, Sc and Zr are added together, a remarkably good recrystallisation resistance was observed as only a thin surface layer had recrystallised after 1hr at 600°C (Table 4). Forbord et al [5] has previously shown that an Al-1wt%Mn-alloy with similar contents of Sc, Zr, Si and Fe as in these alloys resisted recrystallisation at temperatures up to 600°C, even though the dispersoid density was lower than the ones observed in alloys 3-4. This indicates that other alloying elements need to be present in order to stabilise the structure properly. It is well known that Mn forms Al_6Mn dispersoids which also will contribute to the recrystallisation resistance. Mn in solid solution will also exert a drag force on the moving subgrain boundaries.

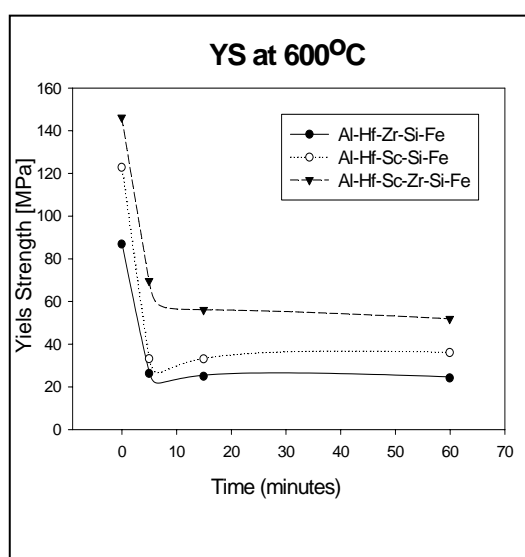


Figure 4: Yield strength at 600°C for alloys 2-4.

3.4 Mechanical Tests.

After extrusion alloy 2-4 was subjected to a high temperature 600°C annealing for up to 1 hour and the yield strength was measured, see Fig.4. The as extruded (0 min) strength naturally increases with increasing alloying content. An abrupt drop in strength was observed already after 5 minutes in all alloys, but the yield strength of alloy 4 seems to stabilise at a higher value than the others. This can be related to the higher dispersoid density, see Table 3. It is also worth to notice that alloy 4 maintains strength significantly better than alloy 3, despite the low difference in alloy content (alloy 4 contains 0.06wt% Zr while alloy 3 does not contain this element).

4. Conclusions

1. WDS was used in order to determine the chemical composition.
2. All alloys, with the exception of alloy 1, resist recrystallisation during extrusion. Alloy 1 does not contain enough Al_3Hf -dispersoids in order to stabilise the structure.
3. Alloy 4 containing Hf, Sc and Zr contains an extremely high density of small and homogeneously distributed $Al_3(Hf,Sc,Zr)$. The dispersoid distribution is quite narrow compared to the ones obtained for alloys 2-3, i.e. the dispersoids seem to nucleate simultaneously in alloy 4.
4. Alloy 4 consequently displays a remarkable recrystallisation resistance as recrystallised grains were observed only in the surface after 1 hr. annealing at 600°C
5. Mechanical test shows that alloy 4 also maintains the strength better than alloys 2 and 3.

Acknowledgement

The authors would like to thank Jostein Røyset, Hydro Al, Sunndalsøra, Norway for his assistance with mechanical testing. Financial support from the Norwegian Research

Council through the project; Heat Treatment Fundamentals (Project No 143877/213) is also gratefully acknowledged.

References

- [1] E.Nes, N.Ryum, O.Hunderi, *Acta Met.* Vol.33, No.1, pp.11-22, 1985.
- [2] N.Ryum, *J of Material Science*, Vol.10, pp. 2075-2081, 1975.
- [3] R S.Hori, N.Furushiro, W.Fujitani, Vol 31, No10, pp. 649-654, 1981.
- [4] H.Hallem, B.Forbord, K.Marthinsen, "An Investigation of Dilute Al-Hf and Al-Hf-Si Alloys", To be published in *Materials Transactions B* (Conference proceedings ICSMA-13, Budapest, Hungary (2003)).
- [5] B.Forbord, H.Hallem, N.Ryum, K.Marthinsen, "Precipitation and recrystallisation in Al-Mn-Zr with and without Sc", To be published (Conference proceedings ICSMA13, Budapest, Hungary (2003)).